QUANTUM INFORMATION

Superadditivity of two quantum information resources

Mohamed Nawareg,[1,2*†] Sadiq Muhammad,[1†] Pawel Horodecki,[3] Mohamed Bourennane[1‡]

Entanglement is one of the most puzzling features of quantum theory and a principal resource for quantum information processing. It is well known that in classical information theory, the addition of two classical information resources will not lead to any extra advantages. On the contrary, in quantum information, a spectacular phenomenon of the superadditivity of two quantum information resources emerges. It shows that quantum entanglement, which was completely absent in any of the two resources separately, emerges as a result of combining them together. We present the first experimental demonstration of this quantum phenomenon with two photonic three-partite nondistillable entangled states shared between three parties Alice, Bob, and Charlie, where the entanglement was completely absent between Bob and Charlie.

INTRODUCTION

Quantum entanglement leads to the most counterintuitive effects in physics (*1*, *2*) and an important quantum resource, which plays a central role in the field of quantum information and communication. Therefore, the investigation of entanglement properties of quantum states is crucial. The characterization of entanglement for multipartite and mixed systems is still under intense research (*3*). Entanglement can be easily destroyed by decoherence processes as a result of unwanted coupling with the environment. This uncontrollable interaction introduces noise and transform, for example, maximally entangled states into mixed states. Therefore, it is critical to know which mixed states can be distilled to maximally entangled states with the help of local operations and classical communication (LOCC) and then be valuable again for further information processing (*4*, *5*). It has been discovered that there is a new class of entangled states where no entanglement can be distilled, and it has been called bound entanglement (*6*, *7*). On the contrary, the distillable entanglement is called free entanglement. After this discovery of bound entanglement, the impression was that this type of entanglement is completely useless for quantum information processing. However, it has been shown that, even in the bipartite case, there is an option to pump entanglement of many bound entangled states into one weakly entangled pair to beat the quantum teleportation fidelity threshold that is unbeatable otherwise (*8*). This process is called activation of bound entanglement, and it was the first manifestation of superadditivity of quantum communication resources. Later, it turned out that bound entanglement can lead to various superadditivity of that kind in the multipartite case (*9*). Bound entanglement also turned out to be useful, somewhat surprisingly, for quantum key distillation (*10*) [see the study by Dobek *et al.* (*11*) for an experimental realization], which eventually paved the way to streaking superadditivity or the activation of quantum bipartite channels (*12*) where the channel corresponding to bound entanglement is activated by a 50:50 erasure channel. Independently, it has been shown that multipartite bound entanglement is a useful resource for other quantum communication tasks. Not only can it be superactivated in a specific situation (*13*), one can use it for remote quantum information concentration as well (*14*). It has also been shown that von Neumann measurements on special bound entangled states allow generation of a new classical secrecy phenomenon, which is called multipartite bound information (*5*). All of these make bound entangled states intriguing objects of quantum information, justifying the term "black hole" of the quantum information field in the sense that the entanglement goes in but is impossible to recover because of the nondistillability (*15*). However, because the bound entanglement can be activated as seen above, analogically, one can say the "black hole can evaporate" in the sense that it can become entangled and therefore become useful.

Here, we report on the first experiment when, metaphorically speaking, "adding two zeros" results in a "nonzero value" or when, in more precise words, the resource (a specific type of free entanglement), which is completely absent in any of the two ingredients, emerges as a result of putting the two ingredients together. Here, the three-partite bound entangled state has been synthesized, and after the interaction with some special free entangled state, the new quantum entanglement has been established, which could not be made out of any of the states (or an arbitrary number of copies of them) of each of the two classes alone. This is also the first observation of three-qubit bound entanglement activation. Note that, at the same time, we experimentally produced the first representative of bound entanglement that can be used for the generation of multipartite bound information (*16*).

It is known that there is more than one type of entanglement in the multipartite case. The most celebrated is the Greenberger-Horne-Zeilinger (GHZ) versus W state nonequivalence (*17*, *18*). In the case of mixed states, there are different types of states that are also not equivalent. Below, we shall describe the situation when one has two different types of mixed state entanglement, each of them unable to perform some task; however, the combination of the two resources (in terms of local interaction and classical communication) resolves this impossibility.

RESULTS

Multipartite bound entanglement

Consider the family of tripartite states $\rho = \rho^{ABC}$ for which the partial transposition of the indices on the, say, first system is positive; that is, one has the nonnegative eigenvalues of partially transposed matrix ρ^{Γ_A} produced from the matrix representation of the original state with the elements $[\rho_{ij,kl,mn}] = [\rho^{ABC}]_{ij,kl,mn}$ by swapping the first two indices corresponding to the row and column of the first subsystem A, namely, $[\rho_{ij,kl,mn}]^{\Gamma_A} = [\rho]_{ji,kl,mn}$. This is just a positive partial transpose (PPT) test attributed to Peres (*19*) performed with respect to system A. Note

[1]Department of Physics, Stockholm University, S-10691 Stockholm, Sweden. [2]Institute of Theoretical Physics and Astrophysics, University of Gdańsk, PL-80-952 Gdansk, Poland. [3]Faculty of Applied Physics and Mathematics, Gdańsk University of Technology, PL-80-233 Gdansk, Poland.
*On leave of absence from the Department of Physics, Damietta University, Egypt.
†These authors contributed equally to this work.
‡Corresponding author. Email: boure@fysik.su.se

that it means that the partially transposed matrix is a legitimate state. It is known that this property makes it impossible for one to distill, via LOCC, any maximally entangled state between party A (on which transpose was checked) and any of the other parties (B or C), or both [see Horodecki *et al.* (*7*)]. Distilling a maximally entangled bipartite pure state with a subsystem X, requires the PPT condition for the original multipartite state to be violated with respect to X from the very beginning. It must be so because the positivity is conserved under LOCC (*7*). An even more demanding condition follows immediately: Because bipartite entanglement fails PPT test if and only if both of its subsystems fail, then to distill entanglement between the two parties X and Y out of some multipartite state, the violation of the test is needed with respect to each of the two parties X and Y independently; that is, one must have neither ρ^{Γ_X} nor ρ^{Γ_Y} positive. Otherwise, on the basis of the fact that any two-qubit entanglement is distillable (*5*), one may write $\mathcal{D}_{X:Y}(\rho) > 0$ to denote that pure entanglement between X and Y can be distilled. To have distillability of singlets between them, this requirement of simultaneous violation of the PPT condition by the two systems is generally necessary for a multipartite system made of qubits. This fact, which is briefly summarized in Fig. 1, follows from the result stating that any two-qubit state violating the PPT condition is distillable (*5*). Dür and Cirac (*9*) have designed a tripartite state ρ^{ABC} that has the property that two of its partial transpositions, ρ^{Γ_A} and ρ^{Γ_B}, are positive, but the third, ρ^{Γ_C}, is not (see Fig. 2). There is some entanglement in this state (because it violates the PPT entanglement test). However, there is no chance to distill any pure entanglement out of it because there is no pair of qubits that violate the PPT test. Thus, the state is bound entangled and is denoted as

$$\mathcal{D}(\rho_{\text{bound}}) = 0 \tag{1}$$

which expresses the fact that no pure entanglement can be distilled among any number of parties. It does not allow any distillability between any two parties, which we denote, as mentioned before, by writing $\mathcal{D}_{B:C}(\rho_{\text{bound}}) = 0$. This can be easily seen from Fig. 2, where the three-qubit state described above has been symbolically depicted.

Bound entanglement activation

Now, consider the following situation shown in Fig. 2 [see the study by Dür and Cirac (*9*)]. The three parties share the abovementioned three-qubit state $\rho^{ABC}_{\text{bound}}$, which is bound entangled because both $\rho^{\Gamma_A}_{\text{bound}}$ and $\rho^{\Gamma_B}_{\text{bound}}$ are positive. This state satisfies $\mathcal{D}(\rho_{\text{bound}}) = 0$. In particular, the distillable entanglement restricted to parties B and C is also zero

$$\mathcal{D}_{B:C}(\rho_{\text{bound}}) = 0 \tag{2}$$

However, in addition, the parties share another tripartite state $\rho^{A'B'C'}_{\text{free}}$. It has free entanglement with respect to subsystems A' and B' but still has no distillability power with respect to the specified cut

$$\mathcal{D}_{B':C'}(\rho_{\text{free}}) = 0 \tag{3}$$

Originally, the bound entangled state is the following one designed by Dür and Cirac (*9*)

$$\rho^{ABC}_{\text{bound}} = \frac{1}{3}|\Psi_{\text{GHZ}}\rangle\langle\Psi_{\text{GHZ}}| + \frac{2}{3}\frac{P}{4} \tag{4}$$

where the GHZ state $|\Psi_{\text{GHZ}}\rangle = \frac{1}{\sqrt{2}}(|000\rangle + |111\rangle)$ and the projection P projects onto $\{|010\rangle, |011\rangle, |100\rangle, |101\rangle\}$, that is, $|010\rangle\langle 010| + |011\rangle\langle 011| + |100\rangle\langle 100| + |101\rangle\langle 101|$, whereas the free entangled state is defined as

$$\rho^{A'B'C'}_{\text{bound}} = [|\Psi^+\rangle\langle\Psi^+|]_{A'B'} \otimes [|\Omega\rangle\langle\Omega|]_{C'} \tag{5}$$

where one of the states is just a maximally entangled state between A' and B', $|\Psi^+\rangle = \frac{1}{\sqrt{2}}(|00\rangle + |11\rangle)$, whereas $|\Omega\rangle$ is either some qubit state or just a vacuum state (no photon).

Let us stress once again the fact that no pure entanglement between Bob and Charlie parts can be created from an arbitrary number of copies of any of the state ρ_{bound} or ρ_{free}, because these states satisfy Eqs. 2 and 3, respectively. Now, as depicted in Fig. 3, this no-go property disappears when the two states are allowed to be processed together. Then, party A (Alice) performs the joint measurement—projection onto a maximally entangled state or the complement three-dimensional projector. If the measurement is successfully concluded (projection onto singlet), then Alice sends the message to Bob and Charlie who may then verify that they now share some free entangled state that can be further distilled to the singlet form. The probability of Alice's joint measurement that led to a successful projection onto the singlet state is $^2/_3$.

The entanglement verification protocol relies on the PPT test that reports entanglement between Bob's and Charlie's laboratories, but among the specially chosen qubit subspaces $\{|00\rangle_{BB'}|11\rangle_{BB'}|0\rangle_C|1\rangle_C\}$, we omitted the trivial vacuum state $|\Omega\rangle_{C'}$ on system C'. It is well known that non-PPT bound entangled states do not exist in a $2 \times N$ system and that all non-PPT $2 \times N$ entangled states are distillable (*3*). In this sense, we have here the LOCC protocol mapping $\rho_{\text{bound}} \otimes \rho_{\text{free}} \rightarrow \sigma_{\text{free}}$, where Eqs. 2 and 3 show initially zero distillable entanglement between Bob and Charlie with the input states (ρ_{bound} and ρ_{free}) but finally give free entanglement, that is, $\mathcal{D}_{BB':CC'}(\sigma_{\text{free}}) > 0$.

Because the total protocol on Fig. 3—being LOCC—cannot create free entanglement (this is a standard property of LOCC operation), we have to conclude eventually that the condition $\mathcal{D}_{BB':CC'}(\rho_{\text{bound}} \otimes \rho_{\text{free}}) > 0$ must have held initially despite vanishing Eqs. 2 and 3. Thus, as already mentioned, we have here the first realization of the extreme superadditivity of quantum resources, which means that although we have complete absence of some quantum information ingredient (free entanglement between Bob and Charlie) in any of the two resources, when one allows the two of them to interact, the ingredient surprisingly emerges. One of the crucial elements here for which this "something out of nothing"

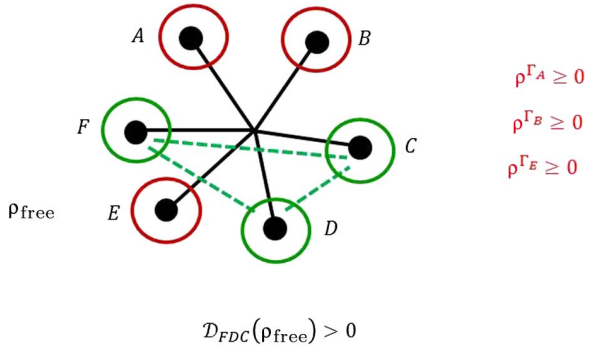

Fig. 1. Two families of qubit states in a six-qubit free entangled state. The red (green) circles symbolize the fact that PPT with respect to the subsystems they mark is satisfied (violated). Only between the pairs with two green circles (marked by green dashed lines) can pure entanglement be distilled if some extra conditions are also satisfied [see the study by Dür and Cirac (*9*) for details].

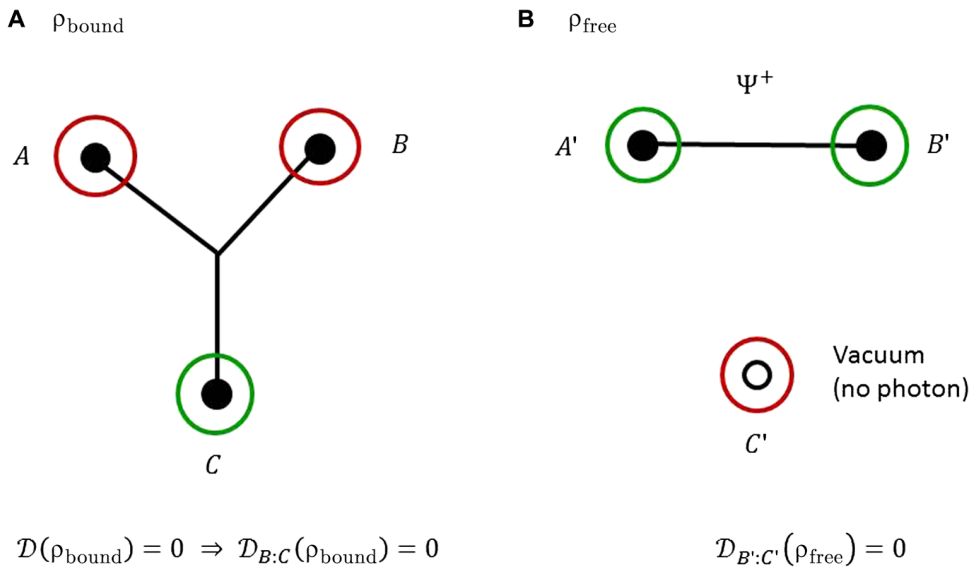

Fig. 2. The two resource states used in the protocol. (**A**) The special bound entangled three-qubit state ρ_{bound} designed by Dür and Cirac (*9*) (see the formula in the main text) is depicted symbolically on the left-hand side. Because there is always at least one qubit guaranteeing a PPT property in each pair of qubits, with the original three-qubit state, there is no chance to distill any pure entanglement out of the state. Thus, distillable entanglement vanishes $\mathcal{D}(\rho_{\text{bound}}) = 0$. In particular, no singlet can be distilled between *B* and *C*, which we write as $\mathcal{D}_{B:C}(\rho_{\text{bound}}) = 0$. However, there is still some entanglement in the state because the PPT test is violated with respect to subsystem *C*. Thus, the state is entangled, and because it is nondistillable, it is therefore bound entangled. (**B**) The second, free entangled state ρ_{free} corresponds to two-qubit singlet and the virtual (vacuum) part. There is no chance to distill entanglement between *B*′ and *C*′ from ρ_{free}. Summarizing the two pictures, no pure entanglement between Bob and Charlie parts can be created from an arbitrary number of copies of any of the state ρ_{bound} or ρ_{free}. In that sense, any of the two states alone is weak because some important quantum entanglement ingredient is completely absent in any of them.

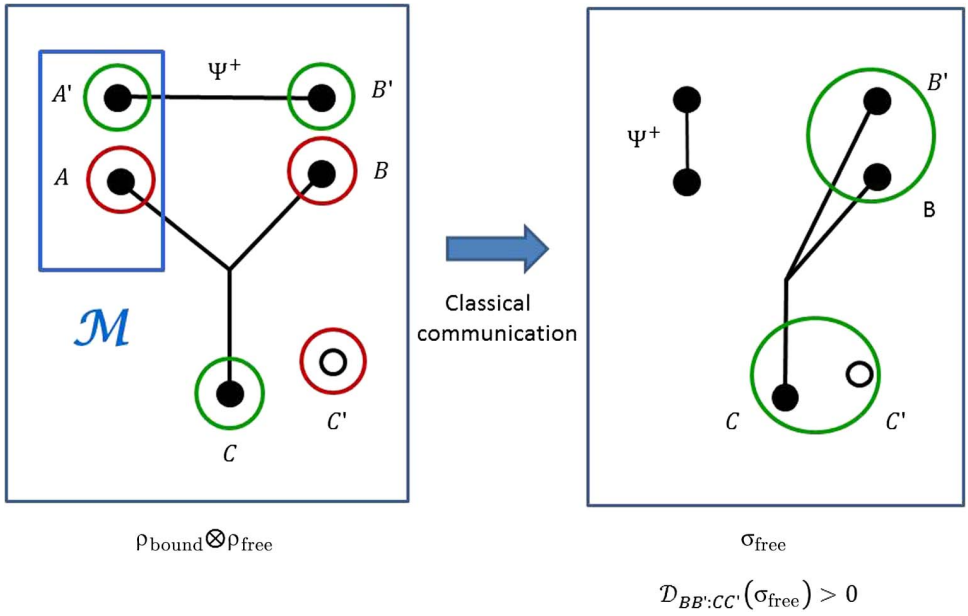

Fig. 3. Superadditivity protocol. The weakness of the two resources shown in the previous picture in Fig. 2 disappears when we allow them to interact through LOCC and the bound entanglement of the first state is activated and creates free entanglement between Bob's and Charlie's part (*BB*′ versus *CC*′). This is the result of Alice's local measurement *M* (projection onto singlet) followed by classical communication to Bob and Charlie about whether the projection was successful. Here, Alice is teleporting to Bob. This emergence of absence before the interaction of free entanglement between Bob and Charlie represents the extreme form of the superadditivity of the two quantum resources. To make a complete description of the consequences of the effect, observe that it implies that given many copies of the two states, one can distill pure singlets among the two parts. Note that because we already have the singlet resource between Alice and Bob, the creation of either *AC* singlet or just full three-partite GHZ is possible (by teleportation from the Bob station provided that he has also some extra copies of particles ρ_{free} at his disposal).

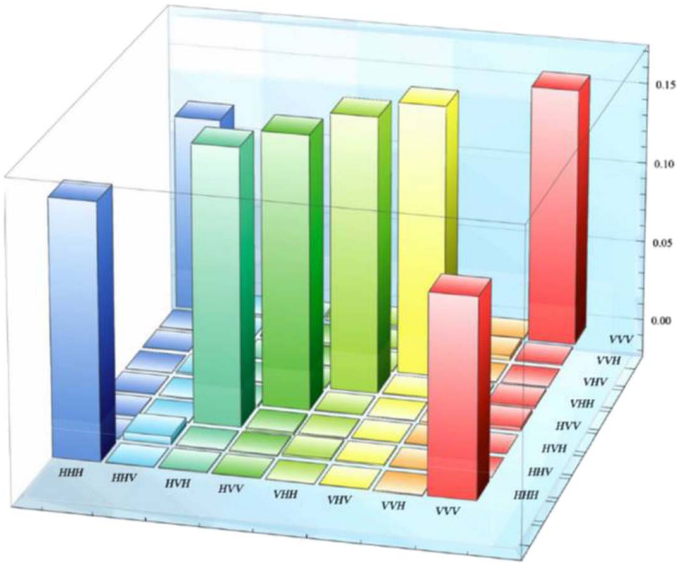

Fig. 4. Experimental results: The density matrix. Density matrix of the mixed three photon bound entangled state ρ^{exp}_{bound} in the computational base $\{|H\rangle, |V\rangle\}$.

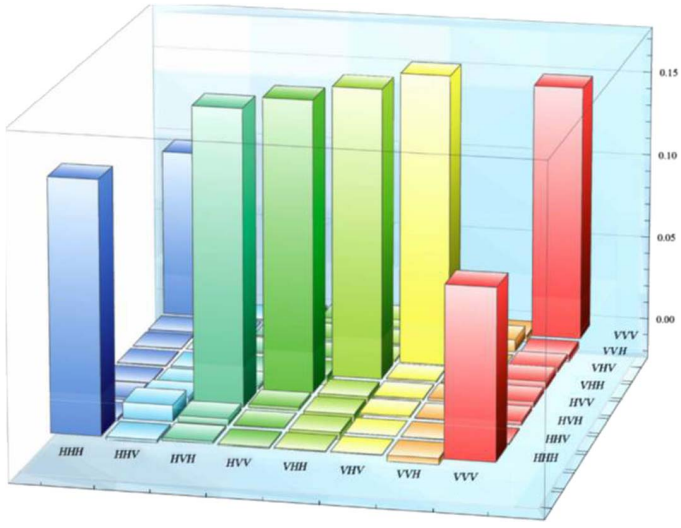

Fig. 5. Experimental results: The density matrix after LOCC operation. Density matrix of the mixed three photon entangled state $\rho^{exp}_{(BB')C}$ in the computational base $\{|H\rangle, |V\rangle\}$.

Table 1. Table of eigenvalues of the partially transposed density matrix of the bound entangled state around *A*/*BC*, *B*/*AC*, and *C*/*AB* cuts. The theoretical eigenvalues are {1/3; 1/6; 1/6; 1/6; 1/6; 0; 0; 0}, {1/3; 1/6; 1/6; 1/6; 1/6; 0; 0; 0}, and {1/6; 1/6; 1/6; 1/6; 1/6; 1/6; 1/6; −1/6} for these cuts, respectively.

A/*BC*		*B*/*AC*		*C*/*AB*	
Eigenvalue	**Error**	**Eigenvalue**	**Error**	**Eigenvalue**	**Error**
0.29098	0.00294	0.29056	0.00287	0.17265	0.00291
0.17086	0.00167	0.17059	0.00140	0.17042	0.00125
0.16787	0.00129	0.16912	0.00180	0.16952	0.00096
0.15968	0.00112	0.15834	0.00148	0.16568	0.00269
0.15537	0.00150	0.15656	0.00184	0.15823	0.00089
0.04764	0.00261	0.04726	0.00267	0.15600	0.00187
0.00485	0.00144	0.00599	0.00155	0.12528	0.00281
0.00275	0.00149	0.00159	0.00149	−0.11778	0.00258

type of effect is to be guaranteed is that one really has to prepare bound entanglement in the experiment. Moreover, this protocol can also be viewed as activation of three-qubit bound entanglement. In this context, we like to mention that there was an unsuccessful experimental attempt to activate four-qubit bound entanglement (*20*).

Finally, it is informative to further examine our protocol from the resource theory perspective governed by the LOCC paradigm (defined by separated locations and quantum operations used as free resources). Namely, at a first look, the protocol presented seems to be viewed as an entanglement swapping experiment transferring the entanglement from B to whatever A was entangled to (in this case, systems B and C). However, this perspective misses the resource framework aspect here, where the locations are essential as dictated by the LOCC paradigm. From this perspective, having just three locations (for example, local regions)—$\tilde{A}$ (with particles A, A'), $\tilde{B}$ (with particles B, B'), and $\tilde{C}$ (with particles C, C')—rather than physical systems is more important. Now, in usual entanglement swapping, it is that one free (distillable) entangled state shared between locations $\tilde{A}$ and $\tilde{B}$ and another free (distillable) entangled state shared between locations $\tilde{A}$ and $\tilde{C}$ initially. After successful joint measurement at $\tilde{A}$, $\tilde{B}$ and $\tilde{C}$ become entangled. In contrast, in our activation protocol, one free (distillable) entangled state is shared between locations $\tilde{A}$ and $\tilde{B}$ and another bound (nondistillable) entangled state is shared between locations $\tilde{A}$, $\tilde{B}$, and $\tilde{C}$, but no entanglement is shared between locations $\tilde{A}$ and $\tilde{C}$, as opposed to the previous case.

Experiment

In our experiment, the physical qubits are polarized photons, where the computational basis corresponds to horizontal H and vertical V linear polarization $|0\rangle = |H\rangle$ and $|1\rangle = |V\rangle$. To prepare the three-photon polarization bound entangled state ρ_{bound}, we used a spontaneous parametric downconversion (SPDC) process and quantum interference. To experimentally and fully investigate the properties of a three-qubit bound entangled state, we have evaluated the three-photon 8×8 density matrix ρ^{exp}_{bound}, by making 27 local polarization measurements in linear, diagonal, and circular polarization bases $|H/V\rangle$, $|+/-\rangle = (|H\rangle \pm |V\rangle)/\sqrt{2}$, and $|R/L\rangle = (|H\rangle \pm i|V\rangle)/\sqrt{2}$. The results of these measurements allow us to tomographically reconstruct the density matrix ρ^{exp}_{bound}. Fourfold coincidences were recorded for each projective measurement.

To guarantee that the reconstruction algorithm does not allow unphysical results, we used a maximum likelihood technique. Figure 4 shows the real parts of the elements of the density matrix ρ^{exp}_{bound} in the H/V basis. We observe the symmetric form of the state in the H/V basis, one peak on each of the four corners and four peaks on the diagonal. The preparation fidelity of ρ^{exp}_{bound} is 95.4 ± 0.3%, and the fidelities of its parts GHZ and projectors are 83.8 and 98.5%, respectively.

In Table 1, we list all eigenvalues of the partially transposed density matrix of the tripartite quantum state ρ^{exp}_{ABC} corresponding to A/BC,

B/*AC*, and *C*/*AB* cuts. For the two first cuts, all the eigenvalues are positive, and in contrast, for the *C*/*AB* cut, one eigenvalue is negative, −0.118 ± 0.003, which implies that the state is bound entangled. The SD of the obtained negative eigenvalue is 64σ (note that the theoretically expected negativity is −0.1667). We have experimentally applied the witness (Eq. 6) to our prepared state ρ^{exp}_{bound}, and we have obtained the result $Tr(w_s\,\rho^{exp}_{bound}) = -0.4785$. The value of the witness for the ideal state bound is $^2/_3$. The difference is due to the imperfect interference in the preparation of the GHZ part of the state. Note that this witness is the one that provides the minimal value (−1) for the maximally entangled state where the Bob qubit subspace is spanned by the two vectors $|HH\rangle$ and $|VV\rangle$ and the Charlie subspace corresponds to the standard basis $\{|H\rangle, |V\rangle\}$.

Table 2. Table of eigenvalues of the partially transposed density matrix of the bound entangled state after activation around the *C*/*BB*′ cut. The theoretical eigenvalues are {1/6; 1/6; 1/6; 1/6; 1/6; 1/6; 1/6; −1/6} for this cut.

Eigenvalue	Error
0.18292	0.00417
0.17648	0.00158
0.17122	0.00174
0.16168	0.00355
0.14714	0.00169
0.14503	0.00177
0.10657	0.00252
−0.09109	0.00274

The superadditivity protocol is performed through a conditional teleportation (with positive Hong-Ou-Mandel interference), where the party Alice performs a joint Bell measurement on modes *A* and *A*′. Figure 5 shows the real parts of the elements of the density matrix $\rho^{exp}_{(BB')C}$ of the state shared between Bob and Charlie in the $\{|H\rangle, |V\rangle\}$ basis. We observe the symmetric form of the state, one peak on each of the four corners and four peaks on the diagonal. The preparation fidelity of exp $\rho^{exp}_{(BB')C}$ is 92.8 ± 0.3%.

In Table 2, we list all eigenvalues of the partially transposed density matrix of the bipartite quantum state $\rho^{exp}_{(BB')C}$ corresponding to the *C*/*BB*′ cut. One can observe that one of the eigenvalues is negative, −0.09 ± 0.003. The SD of the obtained negative eigenvalue is 60σ. These results imply that the state $\rho^{exp}_{(BB')C}$ is free entangled and consequently demonstrate superadditivity of quantum information resources and the bound entanglement activation. We have experimentally applied the witness to the state after activation and have obtained the result, −0.362. Again, this value is smaller compared to the theoretical value of $^2/_3$. The discrepancy is due to the imperfection of the dip interference.

DISCUSSION

We have prepared for the first time a high-fidelity mixed three-qubit polarization bound entangled state. This state is the first experimental

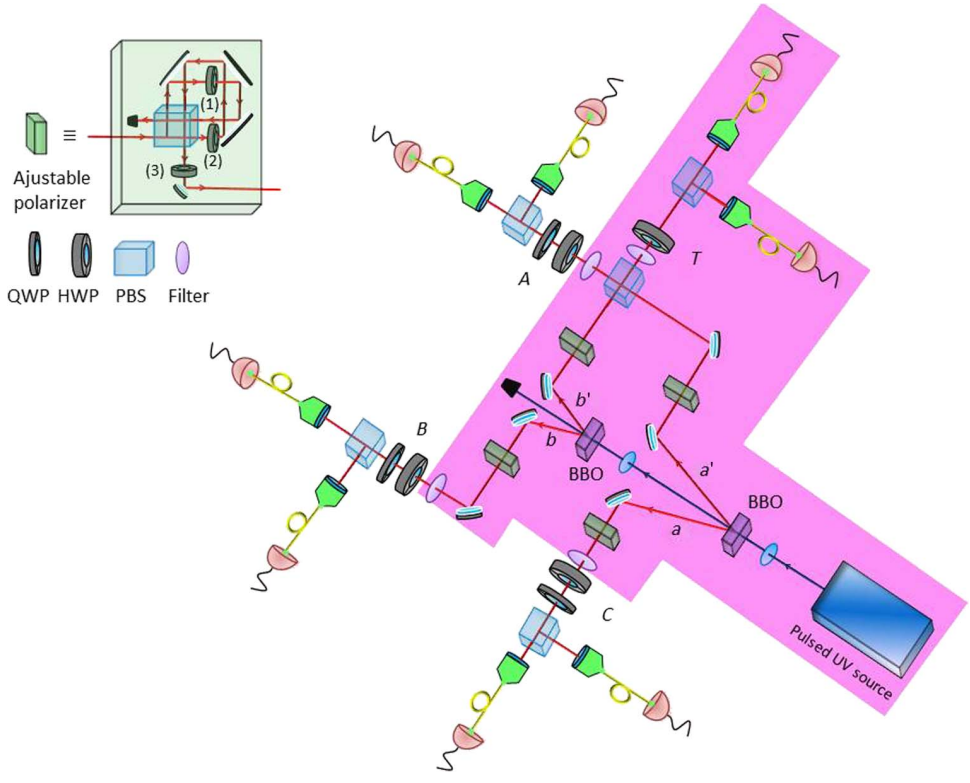

Fig. 6. Experimental setup for the generation of three-qubit polarization bound entangled state. The colored area represents the state preparation. See Methods for more details. QWP, quarter–wave plate; HWP, half–wave plate; PBS, polarizing beam splitter; BBO, β-barium borate; UV, ultraviolet.

realization of a bound entangled state that can be used for generation of multipartite bound information. Using quantum state tomography, we have fully reconstructed its density matrix and demonstrated all its entanglement properties, which make this state useful for novel multiparty quantum communication schemes, for example, secret sharing and communication complexity reduction. We have also realized the activation scheme. The unique feature of quantum mechanics revealed by the present experiment is its something-out-of-nothing character: The ingredient completely absent in any of the two resources suddenly emerges after putting the two resources together. This phenomenon lies in the very heart of quantum information. We strongly believe that the results reported here will help in the development of novel quantum information and communication protocols and in the deeper understanding of foundations of quantum mechanics.

METHODS

The three-photon polarization bound entangled state ρ_{bound} can be obtained as follows: First, we generated the product of two photon pairs in maximally entangled states $|\Psi^+\rangle_{aa'} = (|HH\rangle_{aa'} + |VV\rangle_{aa'})/\sqrt{2}$ and $|\Psi^+\rangle_{bb'} = (|HH\rangle_{bb'} - |VV\rangle_{bb'})/\sqrt{2}$ in modes (a, a') and (b, b'), respectively, by SPDC sources (see Fig. 6) (*21*). The two-photon coincidence rate of these SPDC processes is 2.2×10^5/s, and the fidelity for $|\Psi^+\rangle_{aa'}$ and $|\Psi^+\rangle_{bb'}$ is $96 \pm 1\%$. To prepare the three-qubit $|\Psi_{GHZ}\rangle$, we used the quantum interference at PBS between the modes in a' and b'. To obtain the indistinguishability of the photons in modes a' and b', because of their arrival times, we adjusted the path length of the photon in mode b'. The $|\Psi_{GHZ}\rangle_{ABC} = (|HHH\rangle_{ABC} + |VVV\rangle_{ABC})/\sqrt{2}$ was produced in modes A, B, and C, when the photon in mode T was successfully projected onto the diagonal linear polarization state and conditioned by a click at the trigger detectors in mode T. Second, to prepare the three-qubit mixed state, we placed an adjustable polarizer in each of the four photonic paths a, b, a', and b'. These polarizers consist of a PBS and three adjustable HWP. The settings of these plates for horizontal, vertical, and both polarizations states were (45°,0°,0°), (45°,0°,45°), and (0°,0°,0°), respectively. To switch between the settings, these plates were mounted on motorized rotation stages (see Fig. 6). All these settings were controlled by random number generators to guarantee the needed probability for the preparation of each of the terms of mixed bound entangled state. All measurements in the four modes A, B, C, and T were performed with polarization analysis components followed by single-photon detectors (avalanche photodiode) and a multichannel coincidence unit. The dip interference visibility was 83 ± 1%. The conditioned three-photon coincidence rate was 300/s. For quantum state tomography, the measurement time for each setting was 60 s, which gives an average of 18,000 threefold coincidence events by setting. We note that similar techniques have been used for the preparation of a four-partite bound entangled state (*22*–*24*).

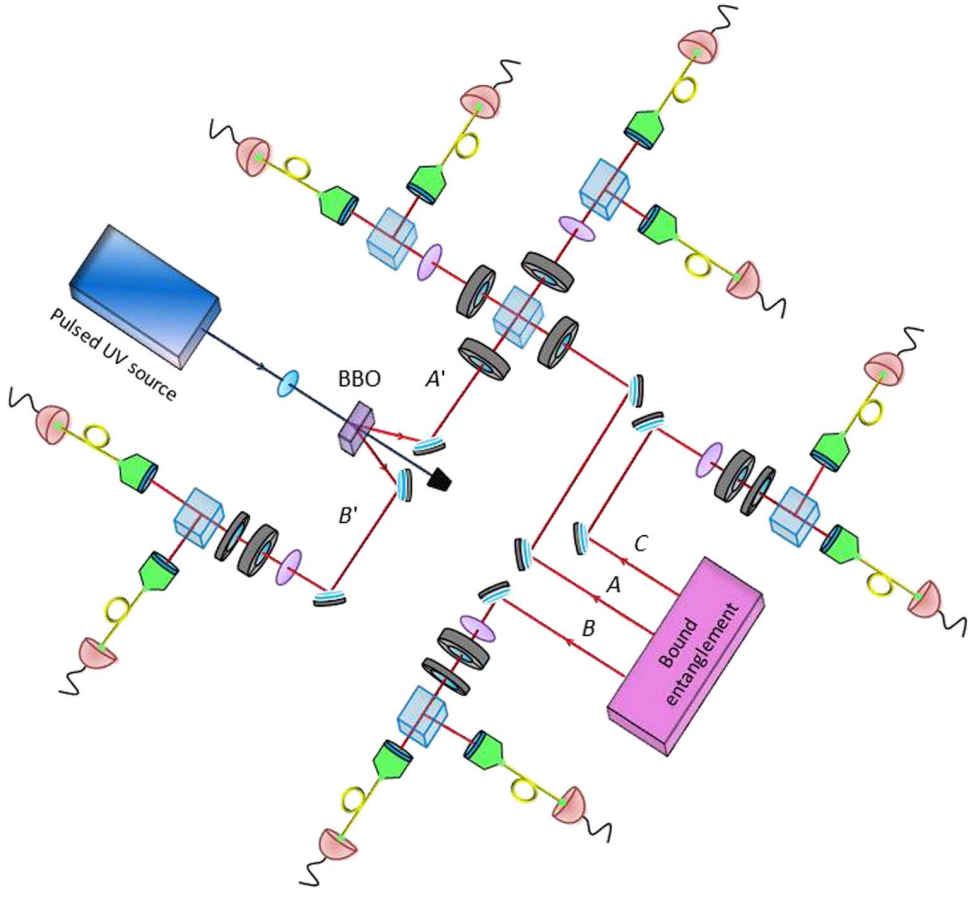

Fig. 7. Experimental setup for the superadditivity protocol. See Methods for more details.

To also check one-qubit/two-qubit separability, we constructed a witness (*25*), with the form

$$\begin{aligned} \mathcal{W}_s = & \frac{1}{2}(\mathbb{1}_A\otimes\mathbb{1}_B + \sigma_A^z\otimes\sigma_B^z)\otimes\mathbb{1}_C \\ & - \frac{1}{2}(\sigma_A^x\otimes\sigma_B^x - \sigma_A^y\otimes\sigma_B^y)\otimes\sigma_C^x \\ & + \frac{1}{2}(\sigma_A^x\otimes\sigma_B^y + \sigma_A^y\otimes\sigma_B^x)\otimes\sigma_C^y \\ & - \frac{1}{2}(\mathbb{1}_A\otimes\sigma_B^z - \sigma_A^z\otimes\mathbb{1}_B)\otimes\sigma_C^z \end{aligned} \quad (6)$$

The activation setup consisted of a quantum interference between the photonic modes A and A' (see Fig. 7). We used a third maximally entangled polarization photon state in modes A' and B' (created by a third SPDC process) and the three-qubit bound entangled state in photonic modes A, B, and C. This interference was realized with the help of PBS and HWP plates set at 22.5°. To obtain the indistinguishability of photons A and A' due to their arrival times, we adjusted the path length of the photon in mode A'. The zero delay corresponded to the maximal overlap with a visibility of $V = 83 \pm 1$ %. The six folded coincidences corresponding to the detection of a photon in each of the six spatial modes B, B', C, T, and two modes after the interference were recorded for each projective measurements. The observed average rate of the six folded coincidences was 1/s. The measurement time for each setting was 1 hour, which gives an average of 3600 sixfold coincidence events by setting.

REFERENCES AND NOTES

1. A. Einstein, B. Podolsky, N. Rosen, Can quantum-mechanical description of physical reality be considered complete? *Phys. Rev.* **47**, 777 (1935).
2. J. S. Bell, On the Einstein-Podolsky-Rosen paradox. *Phys. Chem. Chem. Phys.* **1**, 195–200 (1964).
3. R. Horodecki, P. Horodecki, M. Horodecki, K. Horodecki, Quantum entanglement. *Rev. Mod. Phys.* **81**, 865 (2009).
4. C. H. Bennett, G. Brassard, S. Popescu, B. Schumacher, J. A. Smolin, K. W. Wotters, Purification of noisy entanglement and faithful teleportation via noisy channels. *Phys. Rev. Lett.* **76**, 722–725 (1996).
5. M. Horodecki, P. Horodecki, R. Horodecki, Inseparable two spin-$^1/_2$ density matrices can be distilled to a singlet form. *Phys. Rev. Lett.* **78**, 574 (1997).
6. P. Hoodecki, Separability criterion and inseparability mixed states with positive partial transposition. *Phys. Lett. A* **232**, 333–339 (1997).
7. M. Horodecki, P. Horodecki, R. Horodecki, Mixed-state entanglement and distillation: Is there a "bound" entanglement in nature? *Phys. Rev. Lett.* **80**, 5239–5242 (1998).
8. P. Horodecki, M. Horodecki, R. Horodecki, Bound entanglement can be activated. *Phys. Rev. Lett.* **82**, 1056 (1999).
9. W. Dür, J. I. Cirac, Activating bound entanglement in multiparticle systems. *Phys. Rev. A* **62**, 022302 (2000).
10. K. Horodecki, M. Horodecki, P. Horodecki, J. Oppenheim, Secure key from bound entanglement. *Phys. Rev. Lett.* **94**, 160502 (2005).
11. K. Dobek, M. Karpinnski, R. Demkowicz-Dobrzański, K. Banaszek, P. Horodecki, Experimental extraction of secure correlations from a noisy private state. *Phys. Rev. Lett.* **106**, 030501 (2011).
12. G. Smith, J. Yard, Quantum communication with zero-capacity channels. *Science* **321**, 1812–1815 (2008).
13. P. W. Shor, J. A. Smolin, A. V. Thapliyal, Superactivation of bound entanglement. *Phys. Rev. Lett.* **90**, 107901 (2003).
14. M. Murao, V. Vedral, Remote information concentration using a bound entangled state. *Phys. Rev. Lett.* **86**, 352–355 (2001).
15. B. M. Terhal, M. M. Wolf, A. C. Doherty, Quantum entanglement: A modern perspective. *Phys. Today* **56**, 46–52 (2003).
16. A. Acín, J. I. Cirac, L. Masanes, Multipartite bound information exists and can be activated. *Phys. Rev. Lett.* **92**, 107903 (2004).
17. W. Dür, G. Vidal, J. I. Cirac, Three qubits can be entangled in two inequivalent ways. *Phys. Rev. A* **62**, 8062314 (2000).
18. A. Acín, D. Bruss, M. Lewenstein, A. Sanpera, Classification of mixed three-qubit states. *Phys. Rev. Lett.* **87**, 040401 (2001).
19. A. Peres, Separability criterion for density matrices. *Phys. Rev. Lett.* **77**, 1413 (1996).
20. F. Kaneda, R. Shimizu, S. Ishizaka, Y. Mitsumori, H. Kosaka, K. Edamatsu, Experimental activation of bound entanglement. *Phys. Rev. Lett.* **109**, 040501 (2012).
21. P. G. Kwiat, K. Mattle, H. Weinfurter, A. Zeilinger, A. V. Sergienko, Y. Shih, New high intensity source of polarization-entangled photon pairs. *Phys. Rev. Lett.* **75**, 4337 (1995).
22. E. Amselem, M. Bourennane, Experimental four-qubit bound entanglement. *Nat. Phys.* **5**, 748–752 (2009).
23. J. Lavoie, R. Kaltenbaek, M. Piani, K. J. Resch, Experimental bound entanglement in a four-photon state. *Phys. Rev. Lett.* **105**, 130501 (2010).
24. E. Amselem, M. Sadiq, M. Bourennane, Experimental bound entanglement through a Pauli channel. *Sci. Rep.* **3**, 1966 (2013).
25. M. Bourennane, M. Eibl, C. Kurtsiefer, S. Gaertner, H. Weinfurter, O. Gühne, P. Hyllus, D. Bruss, M. Lewenstein, A. Sanpera, Experimental detection of multipartite entanglement using witness operators. *Phys. Rev. Lett.* **92**, 087902 (2004).

Acknowledgments: We thank R. Horodecki for helpful comments and useful discussions. **Funding:** We acknowledge support from the Swedish Research Council (Vetenskapsrådet), the Knut and Alice Wallenberg Foundation, and European Research Council Advanced Grant QOLAPS. M.N. was supported by the international Ph.D. project "Physics of future quantum-based information technologies" (grant MPD/2009-3/4) from the Foundation for Polish Science. We also acknowledge support from the project Era-Net Chist-Era 7FP UE. **Author contributions:** P.H. proposed and worked out the theory part of the project. M.B., M.N., and S.M. designed the experiment. M.N. and S.M. performed and analyzed the data. M.B. supervised the project. All the authors discussed the results and wrote the manuscript. **Competing interests:** The authors declare that they have no competing interests. **Data and materials availability:** All data needed to evaluate the conclusions in the paper are present in the paper and/or the Supplementary Materials. Additional data related to this paper may be requested from the authors. Correspondence and requests for materials should be addressed to M.B.

Submitted 11 October 2016
Accepted 1 September 2017
Published 22 September 2017
10.1126/sciadv.1602485

Citation: M. Nawareg, S. Muhammad, P. Horodecki, M. Bourennane, Superadditivity of two quantum information resources. *Sci. Adv.* **3**, e1602485 (2017).